# Chapter 1
# Introduction to Gas Hydrates

**Cornelius Borecho Bavoh, Bhajan Lal and Lau Kok Keong**

## 1.1 History of Gas Hydrate

According to Sloan and Koh [1], the research and development of clathrate hydrate, from its discovery to present times, can be classified into three phases. The first phase began in 1778, when Joseph Priestley observed the formation of the $SO_2$ hydrate under laboratory conditions. However, Joseph Priestley did not call it hydrate until 30 years later, in 1811, when Sir Humphrey Davy observed a similar phenomenon in his laboratory with chlorine and water, thus naming it gas hydrates. Since then, hydrates have become an area of interest with regard to scientific laboratory research. The second phase began with the discovery by E. G. Hammershmidt in 1934, suggesting that gas hydrates were the cause of oil and gas pipeline blockages, rather than ice [2]. This began research on the prevention of gas hydrate formation and plugs in oil and gas pipelines. Research on gas hydrate inhibitors increased due to natural gas production and operations higher pressures and lower temperatures conditions.

In the 1960s, a group of Soviet geologists realized the existence of natural gas hydrates in larger quantities in subsea sediments in the tropical, Antarctic Ocean and below the permafrost zones [3]. This discovery commenced the third phase of hydrate research in order to understand natural gas hydrate deposition and develop its production technologies. Interestingly, it has been established that natural gas hydrates possess the potential to become a future energy source to replace fossil fuels [3]. Research has shown that the estimated amounts of natural gas hydrate reserves sit at about $1.5 \times 10^{16}$ m$^3$ which doubles that of fossil fuels [3]. Active research on natural gas production from natural gas hydrate reservoir sources is still ongoing, as a means to develop natural gas production techniques. However, other applications of gas hydrates such as sea water desalination [4], gas storage and transportation [5–7], and mixed gas separation through hydrates for $CO_2$ sequestration [8–15] have been introduced and are still under active research until now. It is hoped that such technologies can be commercialized. Based on the recent rise in climate change issues related to $CO_2$ emissions, hydrate-based $CO_2$ methods to capture and store are on the rise.

## 1.2 Introducing Gas Hydrates

Gas hydrates are ice-like non-stoichiometric compounds which are formed by trapping of gas (guest) molecules into hydrogen-bonded water molecules (host) [1, 16, 17]. They usually form under high-pressure and low-temperature conditions, with the host and guest molecules bonding together via van der Waals forces. A typical gas hydrate structure contains about 85% water molecules, with the water molecules bonded together by hydrogen bonds to form cages which trap the guest molecules [1]. The guest molecule could be liquid or gas. However, the majority of applied and reported guests are typically gases. Some common guest molecules are methane, ethane, propane, carbon dioxide, natural gas, etc. They have similar properties as ice, but differentiate massively in terms of mechanical strength, heat capacity, and thermal conductivity [18, 19]. On the other hand, Tetra-n-butylammonium bromide (TBAB), Tetrahydrofuran (THF), Cyclopentane are the most common liquid gas hydrate formers.

### 1.2.1 Gas Hydrate Structure

Generally, three common types of gas hydrate structures are reported. They are the cubic structure I (sI), the cubic structure II (sII), and the hexagonal structure H (sH) (see Fig. 1.1) [20–22]. The type of gas hydrate structures which is formed is highly influenced by the shape, type, and size of the guest molecule. The shape and size of the hydrate cavities in the cages determine the difference in their structure, while the type and size of the gas molecules accommodated by the water display the type of hydrate formed [19, 23, 24]. Mostly, subsea pipeline flow streams contain methane, propane, and ethane. Therefore, sI and sII are the common hydrate structures formed in oil and gas pipelines [19].

A certain amount of water molecules are required to form each hydrate structure as shown in Fig. 1.1. Generally, all hydrate structures contain small pentagonal dodecahedron ($5^{12}$) cavities as illustrated in Fig. 1.1. Each pentagonal dodecahedron cavity is made up of 12 pentagonal faces. Considering Fig. 1.1, sI consists of a small pentagonal dodecahedral cage ($5^{12}$) and a large tetrakaidecahedral cage ($5^{12}6^2$). The sI small cage has 12 pentagonal faces, and the large cage has 12 pentagonal and 2 hexagonal faces, containing a total of 46 water molecules. The sI cage consists of two small and six large cavities. The sII consists of a small pentagonal dodecahedral cage ($5^{12}$) and a large hexacaidecahedral cage ($5^{12}6^4$). The sII small cage has 12 pentagonal faces, and the large cage has 12 pentagonal and 4 hexagonal faces, consisting of 136 water molecules. The sI cage consists of 16 small and 8 large cavities. The sH has three sizes: the small pentagonal dodecahedral cage ($5^{12}$), the medium irregular dodecahedral cage ($4^35^66^3$), and the large icosahedral cage ($5^{12}6^8$). The sH small cage has 12 pentagonal faces, and medium, 3 square, 6 pentagonal, and 3 hexagonal faces. The large 12 pentagonal and 8 hexagonal faces on the cage consist of 34 water molecules [1, 19]. The sH cage consists of three small cavities, two medium cavities,
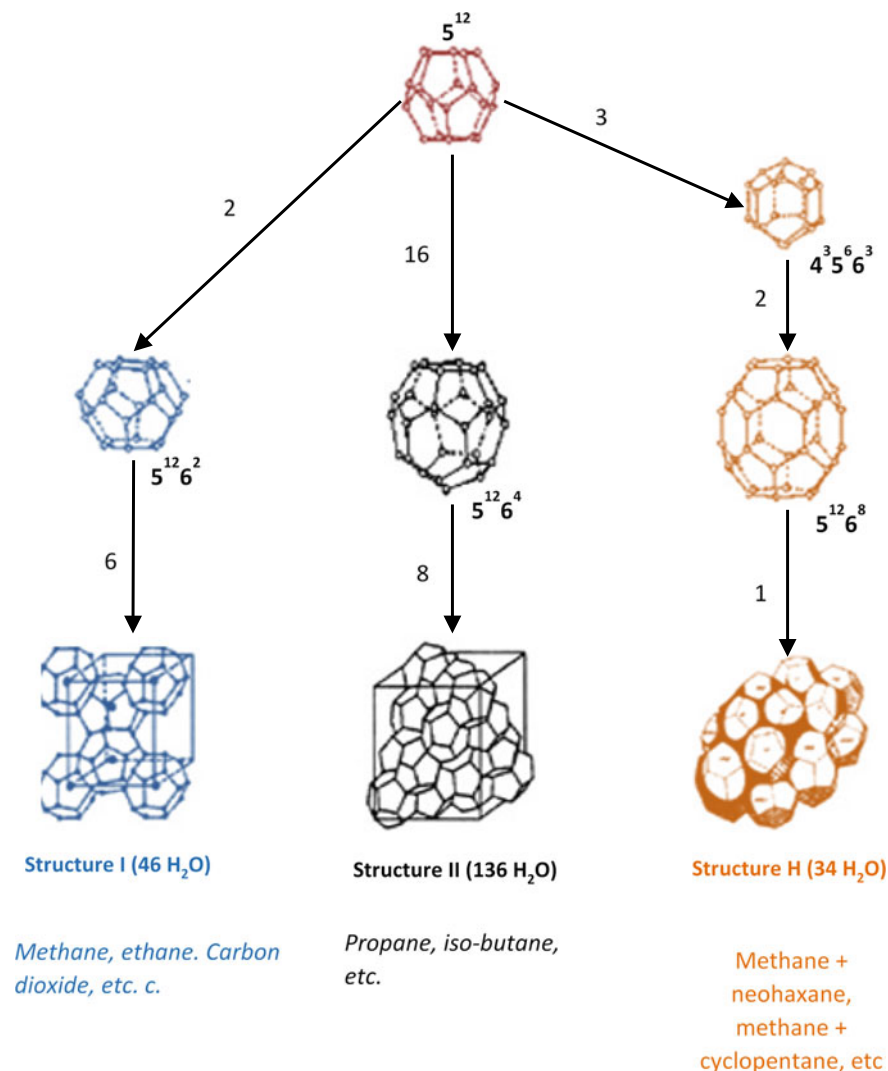
**Fig. 1.1** Details of common gas hydrate structures

and a large cavity. Mostly, the small cavity accommodates one guest molecule, and the larger cavity has two guest molecules with the appropriate size and shape. For the sH hydrate to form, two guest molecules must be present. The gas hydrate cage occupancy by the guest molecules depends on the pressure and temperature.

Interestingly, only small gas molecules <10 Å may probably fill the hydrogen-bonded water cavities. Guest molecules such as carbon dioxide, methane, and ethane have molecular diameters in the range of 4.2–6 A, hence, they usually form sI hydrates. Other gases with molecular diameters less than 4.2 A form sII hydrate structures, for example nitrogen and hydrogen. Generally, the $5^{12}$ cages in the sII

hydrates per volume are 3 times the size of the sI, hence explaining the reason why some smaller molecules such as $N_2$ form sII hydrates and are very stable in such structures [1]. On the other hand, guest molecules with diameters of 6–7 A, such as propane or isobutane, form sII. However, some guest molecules are reported to form more than one hydrate structure. For example, cyclopentane (c-$C_3H_6$) forms either sI or sII hydrates [1]. Nevertheless, guest molecules ranging from 7 to 9.8 A such as cycloheptane or neohexene form sH hydrate structures when they are mixed with smaller gas molecules such as $CH_4$ and $N_2$.

Under the thermodynamic conditions found in oil and gas pipelines, a single guest molecule may occupy one hydrate lattice cavity. However, in some cases, multiple cage occupancies could take place if there are much smaller sized guest molecules in relatively large cavities. Not all hydrate cavities can be occupied with the guest, that is to say, there is no "perfect" gas hydrate crystal. It has been reported that guest molecules such as argon, oxygen, nitrogen, and hydrogen molecules could have multiple cage occupancies.

Generally, the ideal molar gas-to-water ratio for sI, sII, and sH is 1:5 3/4, 1:5 2/3, and 1:5 2/3, respectively. Thus, water molecules are almost always more than the stoichiometric composition with the ideal molar gas–water ratio and full occupancy. This can be simplified as 1:6, considering the inaccuracy in the cage occupancy. This can be fairly observed in the sI hydrate of methane or xenon, which has a hydration number of about 6. The guest-to-cavity ratio is also a major factor accounting for the non-stoichiometry of the cavity filling. Therefore, a perfect non-stoichiometric hydration occurs as the diameter ratio attains unity. No strong forces or chemical bonds exist between the host and the guest molecules; instead, a weak van der Waals force bonds the hydrated structures together. However, the London dispersion forces are the most dominant among the molecules with temporal dipoles. This is much more evident in the presence of the hydrates, which are formed between non-polar natural gas molecules and water. For instance, the total bond energy of the interaction between the water and the methane in simple methane hydrates consists of about 87% London dispersion forces [25].

For every hydrate structure, the thermodynamic (macroscopic) properties are very critical. Therefore, hydrate structural changes adversely affect its thermodynamic conditions. For example, the addition of propane to methane changes the methane hydrate structure from sI to sII. This consequently changes the phase behaviour of methane to suit the new structural stability. When this happens, propane molecules aid to stabilize the large cavity ($5^{12}6^4$) of the structure for two hydrates. This results in a huge drop in the hydrate equilibrium pressure [25]. Interestingly, a mixed hydrate between methane and ethane is expected to form the sI structure, since both of them are sI hydrate formers. However, a transition in their phase behaviour mostly occurs at certain ethane concentrations (below 0.25–0.28 mol fraction of ethane in the mixture), resulting in sII hydrates [25]. This structural transformation is attributed to an unfavourable partitioning condition between the large and the small cavities in the sI hydrate (2:6, respectively).

It has been reported that sI and sII hydrates can coexist during methane hydrate formation. It is believed that there is a rapid $CH_4$ diffusion on the interface of both these hydrate structures [26]. Apart from the structural transformation and coexistence, the variation in sI and sII polyhedral cages also coexists with different non-stoichiometric ratios. Similar observations were confirmed via molecular dynamic simulations by Jacobson et al. [27]. The enthalpy of the dissociation ($H_d$) of the hydrate is another example of microscopic properties which disrupt the macroscopic behaviour of the hydrate formation. The enthalpy of dissociation ($H_d$) is not only associated with the density of the hydrogen bonds, but also associated with the hydrate cavities' cage occupancy. When both large and small cages are filled, $H_d$ decreases, compared in cases where only the large cages are filled. This suggests that an increased hydrate cage occupancy guarantees easier hydrate structure disassociation with less heat. An increase in pressure and guest concentrations could increase the hydrate cage's occupancy. It is important to note that $H_d$ might remain constant with increased hydrate stability with lower dissociation pressure and/or higher dissociation temperatures. This is because the hydrate's lattice stability is dependent on the hydrate's dissociation time with pressure reduction. Therefore, hydrate remediation would be efficient with reduced hydrate lattice stability. Hence, a good understanding of the gas hydrate's lattice stability is very important for hydrate risk management in oil and gas flow assurance fields.

### 1.2.2 Hydrates Verse Ice

It is believed that gas hydrates have very high amounts of water in their structures. Hydrate structures contain about 85% of water, which makes them relatively comparable to ice in properties. Gas hydrate hydrogen bonds are longer than ice by 1% [25]. Much more details of the differences between hydrates and ice can be found in the book by Sloan [1]. However, the major variations in hydrates and ice are in their mechanical and thermal properties. Ice has less mechanical strength than that of hydrates. According to Durham et al. [28], methane hydrate structures are about 20 times stronger than ice. It was summarized that this is because the rate of water diffusion in hydrates is two orders of magnitude lower than that of ice. In addition, the thermal conductivity of sII and sI hydrates (~0.5 W $m^{-1}$ $K^{-1}$) is significantly smaller than that of ice Ih (~2.2 W $m^{-1}$ $K^{-1}$) [29]. Similarly, hydrates have a higher heat capacity (~2100 J $kg^{-1}$ $K^{-1}$), which is much more than ice Ih (~1700 J $kg^{-1}$ $K^{-1}$) [30].

### 1.2.3  Gas Hydrate Formation

The basic requirements necessary for hydrate formation are lower temperature, high pressure, the presence of guest molecules, and the desired amounts of water molecules. The formation process is not chemical, but physical in nature, and no chemical bonds exist between the guest and the water molecules. It must be stated that the guest molecule rotates freely within the cavities of the water molecules. Gas hydrate formation is a crystallization process, which consists of nucleation and crystal growth processes, followed by a massive accumulation process as described in the following subsections.

### 1.2.4  Gas Hydrate Nucleation Process

Gas hydrate nucleation is a microscopic phenomenon, which consists of a tiny number of molecules. This process refers to the formation and growth of hydrate nuclei into a critical size for further growth. Hydrate nucleation is characterized by induction time determination (the time elapsed during which the nucleation processes take place, which includes the formation of gas–water clusters and their growth into stable nuclei with a critical size) [1]. It is a stochastic and time-dependent process and can last from seconds to hours or days, depending on the mixing conditions, composition, apparatus, etc. The stochastic nature of hydrate formation is a result of the degree of metastability (the ability of a non-equilibrium state to persist for a long period of time) that exists in the formation process.

Hydrate nucleation is usually known as a primary nucleation, because the nucleation takes place from freshwater and guest systems. Thus, there is no hydrate formation history or particles in the system. During hydrate nucleation, water molecules group around the guest molecules to form incomplete or complete crystal embryos. These embryos continuously form and shrink due to local mass, pressure, and temperature changes. The mechanism makes the nucleation hydrate a free energy-dependent and statistically random process. When the hydrate nuclei achieve a critical size, the free energy barrier is overcome, and next stage in nucleation is initiated for further growth. During the nucleation process, stage factors such as energy barrier, driving force, critical size, and nucleation rates are very important.

The hydrate formation nucleation and the metastability of gas hydrates can be well understood by observing the pressure and temperature plots in Fig. 1.2. In Fig. 1.2, AB represents the hydrate equilibrium curve, and CD is the so-called thermodynamic spinodal curve that defines the metastable limit. In the metastable region of Fig. 1.2, the system does not have enough energy to overcome the entropy/enthalpy barrier for the creation of critical-sized nuclei. Hence, in this area, crystallization might be aided by the addition of a seed nucleus/crystal, but not without. At point *P*, which acts as the formation process, the system is said to be in a superheated state by the amount of *PR*; therefore, hydrate nucleation is impossible. Hydrate nucleation begins rapidly and
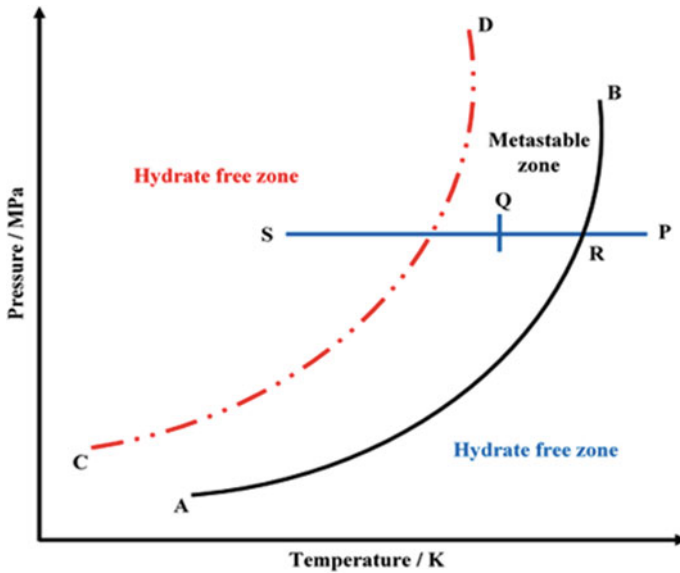
**Fig. 1.2** Hydrate formation as function of subcooling, AB—equilibrium line and CD—spinodal line

crystallizes to the left of the line CD, due to the high driving force. However, between the hydrate equilibrium curve (AB) and the thermodynamic spinodal curve (CD), at point Q, a metastable zone is reached, which is characterized by the possibility to form hydrate nuclei or not to form nuclei. When hydrate nucleation is complete, the cages formed are unstable and can either dissipate or grow to hydrate unit cells, or drive the agglomerations of unit cells, thus forming metastable nuclei.

### 1.2.5 Gas Hydrate Nucleation Mechanism

The solubility of gases in liquid water can give a better understanding of why certain gases form more stable hydrates than others [1]. Previous studies have shown that gas hydrate nucleation takes place at the vapour–liquid interface [1]. To better understand hydrate nucleation processes, the extended model of labile cluster nucleation hypothesis by Christiansen and Sloan [31] becomes important. Their model is based on the fact that water clusters around dissolved gas molecules which may grow to achieve a critical radius, as shown schematically in Fig. 1.3. When a critical size cluster agglomeration is reached, nucleation is said to be complete, which allows hydrate growth to begin.

Generally, gas hydrate nucleation processes can be divided into two types: homogeneous (HON) or heterogeneous (HEN) processes. Homogeneous hydrate nucleation processes take place in systems without impurities. It normally consists of two
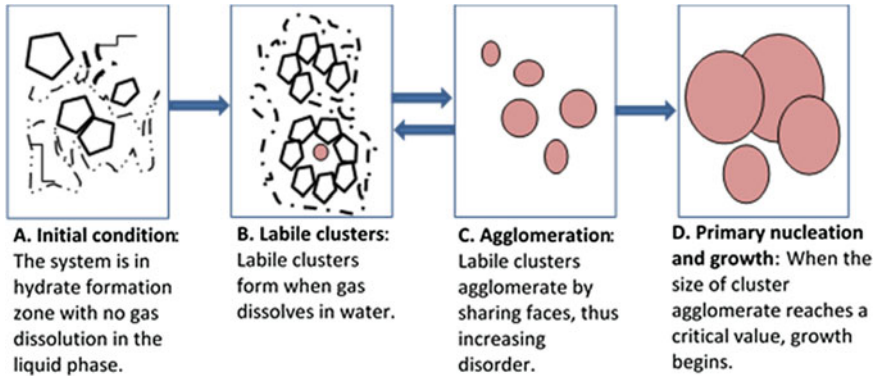
**A. Initial condition:** The system is in hydrate formation zone with no gas dissolution in the liquid phase.

**B. Labile clusters:** Labile clusters form when gas dissolves in water.

**C. Agglomeration:** Labile clusters agglomerate by sharing faces, thus increasing disorder.

**D. Primary nucleation and growth:** When the size of cluster agglomerate reaches a critical value, growth begins.

**Fig. 1.3** Schematic model of the labile cluster nucleation hypothesis

phases: the solute and the nuclei/growing crystal [32]. In real life, it is unusual to observe a HON nucleation process. Gas hydrate nucleation occurs at the gas–liquid interface, which mostly consists of impurities. Also, foreign surfaces such as the reactor/pipe walls might also play an important role in the process. Hence, gas hydrate nucleation processes in real life are generally heterogeneous (HEN). The initial stage of any hydrate study or application is the nucleation stage and thus must be critically considered. However, hydrate nucleation studies are very difficult because it takes place at the molecular level, and are thus considered probabilistic.

The hydrate nucleation phenomenon is controlled by the energy barrier and critical size. Initially, the hydrate embryos form via the battling between the volume excess free energy and the surface excess free energy. Through this process, the surface excess free energy allows solute molecules to participate in the clustering of the subcritical embryos. On the other hand, the volume excess free energy allows solute molecules to fuse into the bulk of the critical-sized hydrate nuclei. Eventually, the existing free energy barrier and critical size of the forming hydrate nuclei develop stable particles with respect to Gibbs free energy, which then drives the hydrate growth progression and hence forms the setting for describing various hydrate nucleation phenomena.

Another important factor worth considering is the driving force. Expressing the hydrate nucleation process of individually clustered embryos or nuclei mechanisms is different from that of the hydrate nucleation driving force at a given pressure and temperature. The clustering embryos are useful to determine the distance from point Q in the metastable area, to the spinodal curve and the label region as shown in Fig. 1.2. At the spinodal point, nucleation assumes a likely occurrence and the chance of nucleation increases with increasing distance from the spinodal curve in the label region. With a sufficient degree of supercooling, and distance in the label region, nucleation becomes spontaneous. Thus, the driving force defines the ability of nucleation and its ability to become spontaneous.

The size of the system can influence the total excess energy needed in a system at any given temperature. Therefore, considering an experimental apparatus with a certain width, the "apparent metastable region", $Q'$, would be somewhat system size and geometry dependent. Ke et al. [25] reported that their hydrate reactor with a diameter of 120 mm demonstrated a fast hydrate nucleation with less subcooling, as compared to reactors with the same diameters, such as 90, 60, and 20 mm. This suggests that decreasing reactor diameter would result in an increase in the degree of subcooling to achieve the required hydrate nucleation. The variation in hydrate nucleation with system size and geometry might be related to the different metastable limits in the reactors itself. However, sample size or amount of water is also system size dependent. However, factors such as system cooling rate, stirring speed, and type were not considered in their discussion. But, their factors also have very serious effects on the hydrate nucleation process.

### 1.2.6 Factors That Enhance Hydrate Nucleation Process

In addition to the condition necessary for hydrate formation, other factors such as agitation cause interfacial gas + liquid + crystal structures to be dispersed within the liquid, giving the appearance of a bulk nucleation from the surface, which affects the resulting hydrate formation. The presence of nucleation sites (such as impurities like sand) and free water may enhance hydrate nucleation or formation. These factors only enhance hydrate formation but are not ultimately necessary for hydrate formation.

### 1.2.7 Gas Hydrate Growth Process

Following hydrate nucleation, hydrate growth takes place. The hydrate crystal growth process depicts the growth of stable hydrate nuclei into solid hydrates. The growth of a hydrate is dependent on the interfacial area, pressure, temperature, agitation, water history, and the degree of supercooling. From Fig. 1.4, the sudden pressure drop caused by the consumption of gas molecules to form hydrate structure depicts hydrate growth and the constant pressure in the system, showing the completion of the formation of hydrates [1]. During hydrate growth, the mass transport of the gas to the hydrate's surface is of major importance and may dominate the process. In addition, the exothermic heat of hydrate formation can also control hydrate growth.

## 1.3 Gas Hydrate Issues

Oil and gas are mostly transported via pipelines from the wellheads to the production site. When these pipelines are operated under thermodynamic (temperature and
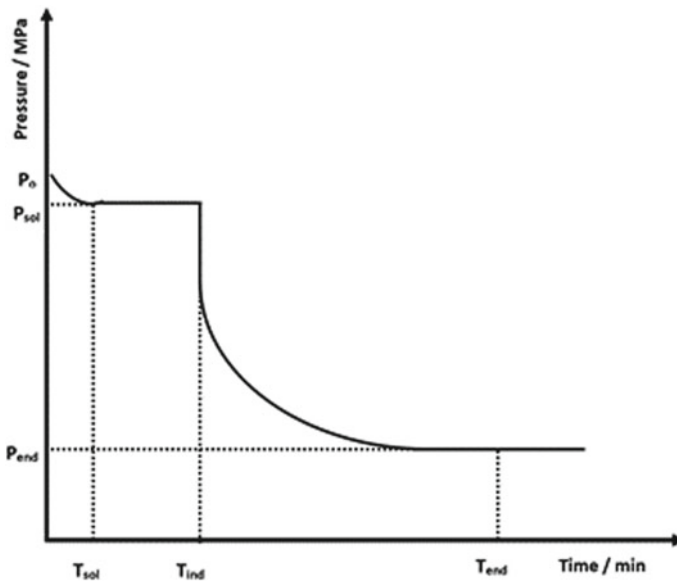
**Fig. 1.4** Schematic representation of the pressure-time plot during kinetic hydrate formation experiment

pressure) conditions which favour hydrate formation, gas hydrate may form in them and may plug the pipelines in severe cases [19].

Gas hydrates form and plug transmission pipelines, resulting in uneconomical operation, conditions, and production stoppages, as well as loss of lives in severe cases. At times, production facilities and drilling operations may also experience hydrate plug issues, especially in deep-sea operations. According to Li et al. [33], the cost of preventing or removing hydrate blocks from pipelines is estimated to over US$200 M annually. Hydrate formation does affect the industry not only economically, but environmentally as well, and can lead to loss of human lives and reduction or stoppages in production. As petroleum activities move into deeper offshore areas, where temperature and pressure conditions are favourable for hydrate formation, especially in the Gulf of Mexico, the Caspian Sea, the North Sea, and permafrost regions like Alaska, the gas hydrates continue to be a major problem that must be mitigated for safe operations to take place.

In view of this, the oil and gas industries have continuously attempted to develop and modify technologies to mitigate hydrate formation.

The available methods for gas hydrate mitigation are water removal, heating, depressurization, and chemical injection [34–36]. Even though these are the available methods, some are not practical in real-world situations, especially with respect to water removal. Some are also expensive, leading to their difficulty in application. Therefore, injection of chemical inhibitors is most commonly applied in the industry [36].

Water removal is the best mitigation method for gas hydrates because once water is completely taken out of the flow stream, no hydrate will form. However, this is only true ideally. It is not practical to completely remove water from the hydrocarbon flow stream. The heating method focuses on the mechanism of using electric heaters to keep the pipeline temperatures in the non-hydrate formation region (i.e. increasing temperature). It is mostly used to keep pipeline temperatures higher during shutdown periods and can also be applied to melt hydrates when the pipeline is plugged [34]. The electric heating method is comparatively more expensive. Moreover, depressurizing pipelines in order to lower the pressure below the hydrate formation pressure is not a suitable method for industrial processes, since it may decrease the energy density to a point that is not economical. So, this method is mostly used to dissociate hydrates after gas hydrates are already formed, and there is a necessity to carry out hydrate plug removal during long shutdowns. The process is very slow and can last for longer periods [34].

Chemical inhibition consists of different inhibition techniques. The first group of chemical inhibitors that are used are thermodynamic inhibitors (THIs), such as alcohols (mainly methanol and glycol). They have been in use for several years. These primarily inhibit gas hydrate formation by depressing the freezing point. The major limitation of thermodynamic inhibition is the large amounts of methanol or glycol required (often more than 20 wt% of the aqueous phase) [32, 33]. In addition, alcohols can cause safety problems since they are highly flammable liquids. It is worth noting that these chemicals are also not environmentally friendly and biogradable. Due to these challenges, new chemical inhibitors were introduced in the 1990s, also known as low-dosage hydrate inhibitors (LDHIs). There are two types of LDHIs, which are anti-agglomerates and kinetic hydrate inhibitors (KHIs). The latter mainly inhibits hydrates by delaying the hydrate nucleation time and is mostly polymers (PVP), while the former allows hydrates to form, but prevents them from agglomeration. One advantage of LDHIs is that they are used at low concentrations (<2 wt%) and have been successfully used in the industry over several years. However, as the oil and gas offshore activities move deeper, these inhibitions face challenges at high subcooling temperatures. Therefore, there is a need for the development of new inhibitors. Recently, ionic liquids (ILs) have been introduced as a dual functional gas hydrate inhibitor (i.e. they have the ability to delay hydrate formation and growth and also shift the equilibrium hydrate curve to low-temperature and/or high-pressure regions) [24, 35, 37–45]. Most recently, natural amino acids and biomolecules have been proposed as novel gas hydrate inhibitors [46–48]. However, less inhibition impact has been observed as compared to the conventional hydrate inhibitors. Research on these novel inhibitors is still at the early stages and is ongoing to discover a less expensive, environmentally friendly, and effective gas hydrate inhibition impact. Chapter 2 gives much more details and the state-of-the-art depictions with regard to the performance associated with recent novel inhibitors (ionic liquids, amino acids, and biomolecules).

## 1.4 Potential Application of Gas Hydrates

Gas hydrate is a potential technology prospect for the future with several important applications in energy, water, and environment research domains. Some known and established applications of gas hydrates are natural gas production, energy storage, gas separation, cold energy storage, $CO_2$ sequestration, energy transport, and desalination applications. These applications generally require gas hydrate formation across various systems to have an efficient and fast hydrate formation, with low energy applications and effective separation factors.

### 1.4.1 Hydrate as Energy Source

There are large amounts of methane gas hydrates forming as solids in sediments and sedimentary rocks within 2000 m of the earth's crust in the permafrost and deep-water regions [49]. Interestingly, it has been established that natural gas hydrate is the next potential future energy source that will replace fossil fuels. Research has shown that the estimated amount of natural gas hydrate reserves (about $1.5 \times 1016$ m$^3$) in the world doubles that of fossil fuel [3]. The estimated amount of natural gas hydrates varies considerably. However, a realistic estimate is that 1016 m$^3$ of methane exists in hydrate form. The reserves of methane hydrate pose to be more than the conventional natural gas reserves and support the recent commitment to economically produce methane hydrates. Since its discovery, the subject of in situ gas hydrates immediately attracted the attention of a wide range of researchers because of its huge quintiles and energy potentials, its possible climate impact, and the drilling and production problems associated with in situ hydrates. Recently, there has been lots of research works to carry out drilling and produce natural gas hydrates, with countries such as the USA, Japan, China, India, making some great progress in that regard.

### 1.4.2 The Capture and Sequestration of Carbon Dioxide

The effects of industrial emission of $CO_2$ and its impact on the environment leading to global warming as claimed in the literature have gained importance in recent years. The main sources of carbon dioxide emissions in the atmosphere are manufacturing industries including cement, iron, and steel making. Thermal power generation and petrochemical industries also contribute massively to the emission of $CO_2$ in the atmosphere [50]. $CO_2$ capture and sequestration are now key areas of active research across many industrialized countries in a bid to conquer global warming. Moreover, the basis of $CO_2$ is to capture $CO_2$ not only as a polluting greenhouse gas, but also as an important raw material. Currently, available techniques for $CO_2$ capture and

separation are handled using chemical solvents, adsorption, chemisorptions, absorption, and chemical bonding through mineralization. However, due to the amount of chemicals used, environmental concerns, and cost, the application of these $CO_2$ capture methods is limited. Therefore, the development of new less energy-intensive processes is of major research interest. The gas hydrate crystallization techniques have certain advantages, as the major chemical needed for $CO_2$ hydrate formation is water, thus providing cheaper and greener chemical applications, as water is very common and is known as a potential chemical for life. Interestingly, the use of gas hydrate promoters can lower the energy demands for hydrate formation [11]. After separation, the capture of carbon dioxide must be sequestered. Similar to hydrate inhibition, there are two types of gas hydrate promoters. Thermodynamic promoters such as THF [51] and acetone [52] are used to shift the behaviour of the hydrate phase boundary. In addition, kinetic hydrate promoters are used to enhance the hydrate formation kinetics. A well-known kinetic promoter is SDS [53]. On the other hand, QAS such as TBAB [54] is known as semi-clathrate hydrate and is also known to be a thermodynamic promoter. Due to the ineffectiveness and environmental concerns, nanoparticles [55] and amino acids [48] have been introduced as a source of good kinetic hydrate promoters comparable to SDS. Chapter 3 deals with much more current developments in the field of hydrate promoters which are available across the literature works.

### 1.4.3   Natural Gas Storage and Transportation

Gas hydrate can also be employed for the transportation and storage of natural gases [56]. This is possible because of the high gas storage capacity of hydrates. It is believed that 1 m$^3$ gas hydrate can store about 180 m$^3$ of gas, which provides a high gas concentration storage [57]. Natural gas hydrate (NGH) is regarded as an important technique among several methods for transporting gas from production fields to the place of use, which includes pipeline natural gas (PNG), liquefied natural gas (LNG), compressed natural gas (CNG), gas to liquid (GTL), gas to commodity (GTC), and gas to wire (GTW), i.e. electricity. Storage and transportation of natural gases in the form of gas hydrates have an economic advantage mainly because of the lower investment in infrastructure and equipment [56]. The key to NGH storage and transportation is to overcome longer induction times and accelerate the hydrate formation. A great deal of research has been done to increase the hydrate formation rate via hydrate promoters, including adding surfactants, stirring, bubbling to the solution [50]. However, the economic aspect remaining is the separation factor in determining the optimal process efficiency. The review of hydrate-based application in gas storage and transportation was presented by Veluswamy et al. [56].

### 1.4.4  Cool Storage Application

The increasing demand of electric power for residential air conditioning and the depletion of the ozone layers by chlorofluorocarbons (CFCs) have brought about an emphasis on using alternative cool storage systems which shift this demand to off-peak periods and eliminate the need for using conventional refrigerants such as chlorofluorocarbons (CFCs) and hydrofluorocarbons (HFCs) [58]. $CO_2$ hydrate is an alternative way for the refrigeration process in the form of clathrate hydrate slurries which acts as a two-phase (solid–liquid) refrigerant. These two-phase refrigerants have a high latent heat of fusion (sometimes also known as phase change materials), which are much more energy efficient than the single-phase refrigerants. $CO_2$ hydrate slurries are promising systems in the field of cold distribution and storage as phase change materials due to the fact that the melting temperatures of some of these clathrate hydrates are consistent with the temperature needed in applications, such as air conditioning. Instead of using mechanical methods, the heat of dissociation of $CO_2$ hydrates can be generated by direct gas injection into an aqueous solution as in the case of ice slurries. The heat of dissociation of these slurries has been found to be suitable for its application in refrigeration [59].

### 1.4.5  Desalination

Most countries have clean water challenges though they have lots of sea water which contains salts. In addition, the oil and gas industry generates large volumes of produced water. The quantities of water are constantly increasing because mature fields have much larger water-to-oil ratio than new fields in production. The produced water is usually saline (30–300 g/L of total dissolved solids). This high salinity restricts their disposal options on shore and also becomes an obstacle to recycling or reuse of the water. Since hydrates are formed between water and gas, both sea and produced water can be treated using hydrate-based promoters.

In this process, the pure water molecules, now in solid form (hydrate), can be recovered by melting and separation which leads to desalination. This method has been long studied in the past using methane hydrate or carbon dioxide hydrate. For different technical and economic reasons, no real industrial solutions emerged at that time using such gas host molecules. Recent advancements in the research of clathrate promoters have opened the door to more adequate, robust, and cheaper solutions, as opposed to methane or carbon dioxide, for a type of application such as desalination. Linga's laboratory plays a vital role in the desalination studies in recent times, with a patent in which they developed a new experimental method for desalination studies [60, 61]. Similarly, active research on the effects of hydrate promoters is still ongoing to fully implement this technology.

## 1.5   Gas Hydrate Testing Method

This section deals with recent gas hydrate apparatus and techniques used by researchers to test hydrate inhibitors and promoters, thermodynamically and kinetically.

### *1.5.1   Apparatus*

In order to successfully apply gas hydrate-based technologies, a good understanding and evaluation of the formation of kinetics and phase behaviour in gas hydrate promoters and inhibitors are very useful. Generally, authors/researchers employ various forms of techniques to achieve the required hydrate kinetics and phase behaviour. Further details on the apparatus and techniques used for hydrate studies are provided in Sloan's book [1]. However, in recent times, various simulations and experimental apparatus and techniques have been adopted. A high-pressure reactor [62–64], mostly called autoclaves, is the most employed experimental apparatus. However, there have been instances where nuclear magnetic resonance (NMR) microscopy [65], in situ powder X-ray diffraction [22, 46], and ultrasonic equipment have been employed to study the phase behaviour and kinetics of hydrate formation. However, rocking cell and differential scanning calorimetry (HP DSC) [36, 37, 66, 67] are mostly used for hydrate phase behaviour, and the rest are mostly employed for hydrate kinetics, and molecular and structural studies. In addition, some studies have also been conducted using high-pressure flow loops to evaluate the kinetics of hydrate formation [68, 69]. Another technique that has been used for kinetic studies is the high-pressure automated lag time apparatus (HP-ALTA). This technique offers a wide range to run lots of experiments in a short time [70].

### *1.5.2   Hydrate Kinetic Measurement*

Generally, gas hydrate kinetic studies are based on their applications. However, the methods of measuring hydrate kinetic are similar but the interpretation is solely reserved for the kind of hydrate application under study. The kinetic measurements are based on their formation and disassociation path. Sloan's book gives details on how these quantities are measured; however in this book, we would consider recent hydrate kinetic measurements used by the authors. Kinetic indicators are hydrate nucleation time and rate, growth rate, total gas uptake/consumption, hydrate dissociation rate, hydrate conversion ratio, hydrate preservative ability, etc. Herein, the recent methods used to measure the aforementioned hydrate kinetic indicators are briefly discussed. There are generally two methods for testing hydrate nucleation processes. The first is the nucleation at constant temperature and degree of subcooling,

and the second method involves nucleation during which constant cooling experiments take place. The latter evaluates the subcooling at which hydrate nucleation will happen. The former determines the hydrate nucleation rate and induction time at a specific driving force. Because the subcooling point is less probabilistic at constant cooling, some researchers prefer to use the second method. Generally, at constant subcooling and temperature induction, time measurement is very stochastic and not preferred by some authors. However, it is worth noting that the subcooling point method is also stochastic in application, since the nucleation time/rate are all dependent on the degree of subcooling. On the other hand, for constant temperature mode, a fixed subcooling is applied in the system. Hence, the nucleation time/rate depends on a function of a time average of observed nucleation time. Also, the cooling rate is known to affect the subcooling point.

Generally, to perform a hydrate kinetic experiment, the cell is initially cooled to temperatures which are about 2 K higher than the hydrate equilibrium temperature. Then, the desired gas/guest is pressurized into the cell up to the desired experimental pressure. The stirrer is turned on, and the system is left to stabilize, after which the system is cooled down to the experimental temperature without stirring during the cooling period. There would be a decrease in the system pressure due to the gas solubility into the liquid phase. When the system pressure becomes constant, at the experimental temperature, the stirrer is turned on. When a rapid pressure drop is noted in the system, the hydrate is assumed to have formed. When the system pressure becomes constant after hydrate formation for more than 3 h, the experiment is considered completed.

### 1.5.2.1   Estimation of Kinetic Parameters

Induction time is defined as the nucleation time or induction time of gas hydrate formation for a noticeable hydrate nucleus crystal to be formed. It is estimated that the time at which a rapid temperature increases, or pressure drop is observed in the system and in a pressure—temperature verse time plot of any hydrate experiment. However, it is also detected via visual observation using a glass window or camera in some set-ups.

The initial rate of hydrate formation is very important for gas hydrate application as mentioned earlier. It describes how fast or slow the hydrate forms in any given system. Usually, a slow hydrate formation rate is preferred in hydrate testing inhibitors, while hydrate promoters are expected to exhibit fast hydrate formation rates. The initial rate of hydrate formation is usually calculated by most authors following Eq. (1.1):

$$r(t) = \frac{n_i^{i-1} - n_i^{i+1}}{t_{i-1} - t_{i+1}} n_{w_0}^{-1} \tag{1.1}$$

where $n_i^{i-1}$ and $n_i^{i+1}$ are the amount of moles of gas in the phase at time $t_{i-1}$ and $t_{i+1}$, respectively, and $n_{w_0}^{-1}$ is the amount of moles of water in the liquid phase.

The amount of gas consumed or total gas uptake is the amount of gas consumed or converted into hydrate, which is useful to understand the amount of gas that can be trapped in the hydrates. In gas hydrate-based applications such as gas storage and separation, the estimation of the total gas uptake is very important. Interestingly, the total amount of gas consumed during hydrate formation is not completely dependent on its formation rate. That is to say, the high rate of hydrate formation does not guarantee high moles of gas consumed and vice versa. However, kinetic hydrate inhibitors are required to reduce the moles of gas consumed during hydrate formation, while kinetic hydrate promoters are expected to enhance it. The real gas equation (Eq. 1.2) is generally adopted to determine the total amount of gas consumed during hydrate kinetic studies. This is valid for isothermal experiments with the assumption that no water volume changes during hydrate formation.

$$n_g = \left[ \left( \frac{PV}{RTz} \right)_0 - \left( \frac{PV}{RTz} \right)_t \right] \tag{1.2}$$

where $P$, $T$, $Z$, and $V$ are the hydrate reactor pressure, temperature, gas compressibility factor, and volume of the gas phase, respectively. $Z$ can be determined by employing any equation states (however, the Peng–Robinson equation of state is mostly used in the literature). $R$ represents the universal gas constant, while the subscript 0 denotes the initial time at which the experiment was started; $t$ denotes anytime $t$ of the experiment. The total gas uptake is usually normalized to eliminate the sample size using Eq. (1.3). In reality, the normalized amount of gas consumed ($n_N$) indicates the total quantity of gas trapped in one mole of a loaded solution.

$$n_N = \frac{n_g}{n_w} \tag{1.3}$$

Storage capacity (SC) is employed in applications such as gas transportation and storage to quantify the amount of gas that can be trapped in any hydrate system. However, it can also be used in also all hydrate kinetic studies for analysis. The storage capacity describes the volume of gas captured under standard conditions (STP) per volume. It can be determined as follows:

$$SC = \frac{V_g^{STP}}{V_H} = \frac{n_g RT^{STP}/P^{STP}}{V_H} \tag{1.4}$$

where $V_H$ is the gas hydrate volume and estimated using Eq. (1.5).

$$V_H = Mn_g v_W^B \tag{1.5}$$

where $v^B{}_W$ is the molar volume of empty hydrate lattice.

$$v_W^B = \left(11.835 + 2.217 \times 10^{-5}T + 2.242 \times 10^{-6}T^2\right)^3$$
$$\times \frac{10^{-30}N_A}{46} - 8.006 \times 10^{-9}P + 5.448 \times 10^{-12}P^2 \tag{1.6}$$

where $P(\text{MPa})$ and $T(\text{K})$ denote the pressure and temperature of the system. $N_A$ is Avogadro's constant. Also, it is assumed that the molar volume of gas hydrate and empty hydrate lattice are the same. Hence, the trapping mechanism of gas into hydrogen water molecules is expressed in the reaction below (see Eq. 1.7):

$$G + M\text{H}_2\text{O} \leftrightarrow G.(\text{H}_2\text{O})_M \tag{1.7}$$
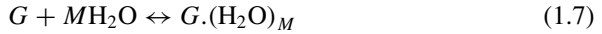
where $G$ is the type of guest and $M$ represents the hydration number. This is linearly related to the fractional cage occupancy. However, this is true for sI hydrates. For sII hydrates, the constant 46 in the equation would be 136.

$$M = \frac{\eta_k}{\sum \upsilon_m \left(\sum \theta_{m,i}\right)} \tag{1.8}$$

where $\eta_k$ is the number of water molecules in a unit cell, $\upsilon_m$ is the number of cavities of type m in the unit cell, and $\theta_m$ is the fractional occupancy of cavity of type m, which are mostly calculated using the Langmuir adsorption theory, as follows.

$$\theta_{m,i} = \frac{C_{m,i}f_i}{1 + \sum C_{m,i}f_i} \tag{1.9}$$

where $C_{m,i}$ represents the gas Langmuir constant of the guest $(G)$ in type i cavity and $f$ denotes the fugacity of the guest $(G)$ in the gas phase. The Langmuir constant of gas $(C_{m,i})$ is given in Eq. (1.10):

$$C_{m,i} = \frac{A_{m,i}}{T} \exp\left(\frac{B_{m,i}}{T}\right) \tag{1.10}$$

$A_{m,i}$ and $B_{m,i}$ are constants. $T(\text{K})$ is the temperature. The fugacity of guest in the gas phase can be determined by any equation of state.

Water-to-hydrate conversion ratio describes the portion of water molecules that is converted to gas hydrate per mole of initial solution. It is very useful in hydrate-based desalinating studies. A high water conversion-to-hydrate ratio would guarantee high water desalination efficacy. Equation (1.11) is usually adopted to calculate the water-to-hydrate conversion ratio.

$$\text{Conversion} = \frac{Mn_g}{n_{w_o}} \tag{1.11}$$

### 1.5.3  Hydrate Dissociation and Preservation Measurements

Dissociation and preservation tests for hydrates are usually performed first by cooling the system. After the hydrate forms in a typical manner as explained in the previous section, the temperature of the reactor is then lowered to the hydrate equilibrium temperature at the pressure which the hydrates are expected to be preserved. Mostly, the hydrate is expected to be preserved at an atmospheric pressure until they are dissociated. Hence, after the reduction in temperature to 263.2 K, the pressure in the reactor is decreased to atmospheric pressure and allowed to stabilize. These experiments are used to determine how stable the hydrate would be especially for $CO_2$ storage and hydrate pellets applications due to climate concerns.

### 1.5.4  Hydrate Phase Behaviour Measurement

In order to measure the hydrate phase behaviour, the isochoric temperature cycle (T-cycle) or pressure search mode is used [23]. During this experimental mode, the reactor is first cleaned and vacuumed. Then, the temperature of the system is set to about 2–3 K above the hydrate equilibrium temperature of the studied experimental pressure. The solution under study is then loaded into the cell, after which the system is compressed with the guest molecules. The system is then left to stabilize while the stirrer is turned on. When the pressure becomes constant, the system temperature is then lowered to an adequate temperature, which would allow hydrate formation. A sharp pressure drop in the system shows hydrate formation. After gas hydrates are formed, the system is heated slowly, stepwise, at about 0.5 K/step for 3 h at each step as proposed by Tohidi et al. [71]. Figure 1.5 illustrates the hydrate formation and dissociation process during hydrate phase behaviour measurement. The hydrate phase equilibrium point is determined as the point where the cooling curve intersects with the heating curve as described in Fig. 1.6.

#### 1.5.4.1  Average Depression Temperature ($\overline{T}$)

The average depression temperature ($\overline{T}$) is calculated using Eq. (1.12) [36]. It is used to quantitatively analyse the impact of hydrate phase behaviour shift in the presence of inhibitors/promoters.

$$\overline{T} = \frac{1}{m} \sum_{i=1}^{m} \Delta T \tag{1.12}$$

where $m$ is the number of data points and $\Delta T$ is the difference between measured hydrate dissociation temperature in the presence of inhibitor and pure water. The
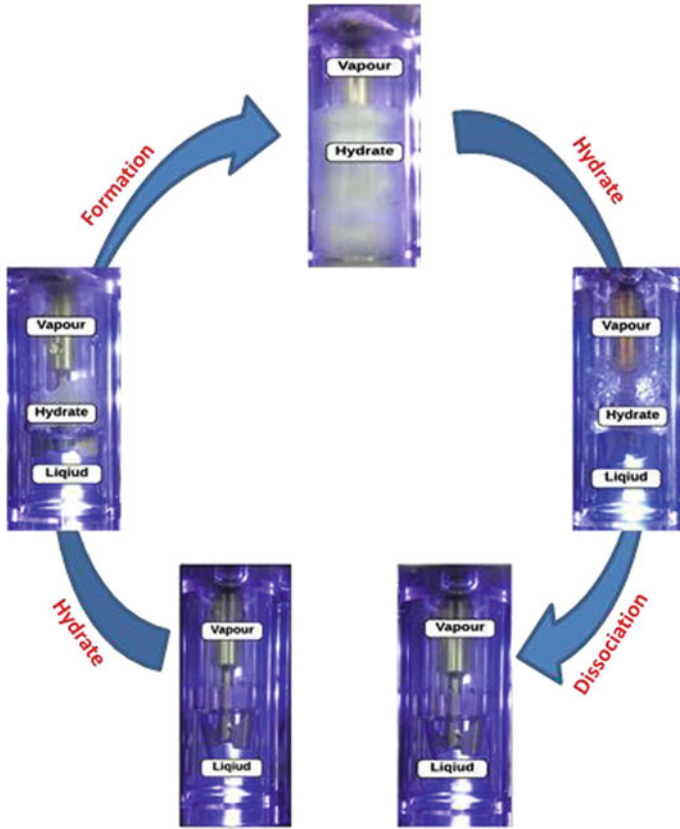
**Fig. 1.5** Pictures of hydrate formation and dissociation

pure water equilibrium temperature can be determined using CSMGem, PVTsim, or any hydrate model at constant pressure [19].

### 1.5.4.2  Calculation of Methane Hydrate Dissociation Enthalpy

Determining of hydrate dissociation enthalpy is critical in understing the hydrate structure and guest cage occupancy, which is related to the relative size of the guest molecule and cavity size. Generally, the gas hydrate formation disassociation enthalpy is defined as the heat required to decompose hydrate and to release one mole of guest gas molecule, with a reaction formula as:
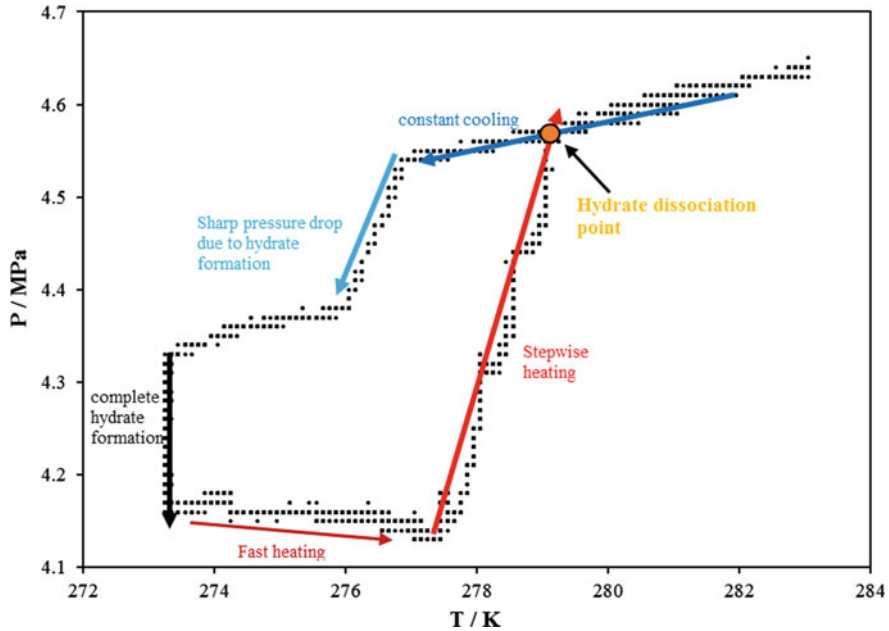
$$M.n\text{H}_2\text{O}_{(s)} = M + n\text{H}_2\text{O}_{(l)} \tag{1.13}$$
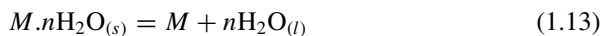
**Fig. 1.6** Typical pressure–temperature profile measured during methane + deionized water experiment

where $M$ and $n$ are the guest and hydration numbers, respectively. The enthalpy of hydrate dissociation can be determined calorimetrically as a direct method or indirectly by using the Clausius–Clapeyron equation via the aid of the measured $HL_wVE$ points. The hydrate dissociation enthalpy is estimated by employing the Clausius–Clapeyron equation (Eq. 1.14) as follows [1]:

$$\frac{d(\ln P)}{d(T^{-1})} = \frac{-\Delta H_d}{zR}$$

(1.14)

where $P$, $T$, $\Delta H_d$, $z$, and $R$ are pressure, temperature, dissociation enthalpy, compressibility factor, and universal gas constant, respectively.

## 1.6 Gas Hydrate Models

Based on the knowledge of hydrate structure and formation mechanisms, effective hydrate thermodynamic and kinetic predictive methods have been formulated by several authors. These predictive models are needed and are constantly modified for more accurate prediction, especially kinetic models.

### *1.6.1   Nucleation and Growth Models*

Hydrate nucleation and growth processes have a lot of measurement challenges, resulting in the difficulty to model their formation processes. However, there has been a rise in the attempts to model hydrate kinetics from the Bostnia days till now. Both nucleation and growth models have been used in literature. Vysniauskas and Bishnoi et al., in their seminal work, reviewed the kinetics of hydrate formation and developed a semi-empirical model to correlate experimental data on methane and ethane hydrate formation. In their work, the hydrate formation modelling did not include the hydrate nucleation. They further followed up with other modifications of their model. Kvamme et al. developed a generic hydrate nucleation model based on the phase field theory for describing the nucleation of $CO_2$ hydrates in aqueous solutions. Other forms of hydrate nucleation and growth theories including CNT have been reviewed in Chap. 4 of this book. However, due to the probabilistic nature of hydrate nucleation and its dependence on apparatus and many other factors, very poor accurate hydrate kinetic prediction has been reported.

### *1.6.2   Thermodynamic Models*

The use of thermodynamic hydrate models has made hydrate formation pressure and temperature prediction much easier for industrial applications. This model has been extended to several hydrate systems and is very accurate in predictions by comparing them with its kinetic counterpart. On the other hand, simple hydrate phase behaviour models can be developed. The model proposed by van der Waals and Platteeuw (1959) discussed the basics of the modern hydrate models with or without inhibitors. Since new hydrate inhibitors such as ionic liquids, and amino acids have been reported, constant modification of the models has been developed to suit such systems. The advantage of this model is that it is able to predict macroscopic property such as pressure. Chapter 4 gives a detailed method of all the hydrate thermodynamic models used recently in the presence and absence of hydrate inhibitors.

## 1.7   The Connection of This Chapter to Those That Follow

This chapter provides a background for hydrate formation and applications. Considering the fact that the focus of this book is to provide recent advances on the progress of hydrate chemical additives, the next chapter will provide the state-of-the-art development on recent hydrate inhibitors devel and their inhibition mechanisms. Similarly, Chap. 3 deals with gas hydrate additives (promoter) that enhance hydrate formation

for gas separation, desalination, and $CO_2$ storage. It also provides the hydrate promotion mechanism for these additives. Lastly, Chap. 4 details the thermodynamic and kinetic models for gas hydrates in the presence and absence of additives, including recently introduced novel additives.

# References

1. Sloan ED, Koh CA (2007) Clathrate hydrates of natural gases, 3rd edn. CRC Press, Boca Raton, p 758
2. Hammerschmidt EG (1934) Formation of gas hydrates in natural gas transmission lines. Ind Eng Chem 26:851–855
3. Englezos P (1993) Clathrates hydrates. Ind Eng Chem Res 32:1251–1274
4. Javanmardi J, Moshfeghian M (2003) Energy consumption and economic evaluation of water desalination by hydrate phenomenon. Appl Therm Eng 23:845–857
5. Javanmardi J, Nasrifar K, Najibi SH, Moshfeghian M (2005) Economic evaluation of natural gas hydrate as an alternative for natural gas transportation. Appl Therm Eng 25:1708–1723
6. Xu C-G, Li X-S (2015) Research progress on methane production from natural gas hydrates. RSC Adv 5:54672–54699
7. Lang X, Fan S, Wang Y (2010) Intensification of methane and hydrogen storage in clathrate hydrate and future prospect. J Nat Gas Chem 19(3):203–209
8. Li S, Fan S, Wang J et al (2009) $CO_2$ capture from binary mixture via forming hydrate with the help of tetra-n-butyl ammonium bromide. J Nat Gas Chem 18:15–20
9. Chun-Gang X, Xiao-Sen L (2014) Research progress of hydrate-based $CO_2$ separation and capture from gas mixtures. RSC Adv 4:18301–18316
10. Duc NH, Chauvy F, Herri JM (2007) $CO_2$ capture by hydrate crystallization—a potential solution for gas emission of steelmaking industry. Energy Convers Manag 48:1313–1322
11. Babu P, Linga P, Kumar R et al (2015) A review of the hydrate-based gas separation (HBGS) process for carbon dioxide pre-combustion capture. Energy 85:261–279
12. Park S, Lee S, Lee Y et al (2013) $CO_2$ capture from simulated fuel gas mixtures using semi-clathrate hydrates formed by quaternary ammonium salts. Environ Sci Technol 47:7571–7577
13. Mohammadi AH, Anderson R, Tohidi B (2005) Carbon monoxide clathrate hydrates: equilibrium data and thermodynamic modeling. AIChE J 51:2825–2833
14. Li S, Fan S, Wang J (2010) Clathrate hydrate capture of $CO_2$ from simulated flue gas with cyclopentane/water emulsion. Chin J Chem Eng 18:202–206
15. Kim SM, Lee JD, Lee HJ et al (2011) Gas hydrate formation method to capture the carbon dioxide for pre-combustion process in IGCC plant. Int J Hydrogen Energy 36:1115–1121
16. Ameripour S (2005) Prediction of gas-hydrate formation conditions in production and surface facilities. Doctoral dissertation, Texas A&M University
17. Harrison SE (2010) Natural gas hydrates. Stanford University, p 4
18. Obanijesu EO, Gubner R, Barifcani A et al (2014) The influence of corrosion inhibitors on hydrate formation temperature along the subsea natural gas pipelines. J Pet Sci Eng 120:239–252
19. Koh CA, Sloan ED, Sum AK et al (2011) Fundamentals and applications of gas hydrates. Ann Rev Chem Biomol Eng 2:237–257
20. Jeffrey GA (1984) Hydrate inclusion compounds. J Incl Phenom 1:211–222
21. Jeffery GA (1972) Pentagonal dedecahedral water structure in crystalline hydrates. Mat Res Bull 7:1259–1270
22. Ripmeester JA, Tse JS, Ratcliffe CI et al (1987) A new clathrate hydrate structure. Nature 325:135–136
23. Partoon B, Wong NMS, Sabil KM et al (2013) A study on thermodynamics effect of [EMIM]-Cl and [OH-$C_2$MIM]-Cl on methane hydrate equilibrium line. Fluid Phase Equilib 337:26–31

24. Tariq M, Rooney D, Othman E et al (2014) Gas hydrate inhibition: a review of the role of ionic liquids. Ind Eng Chem Res 53:17855–17868
25. Ke W, Svartaas TM, Chen D (2019) A review of gas hydrate nucleation theories and growth models. J Nat Gas Sci Eng 61:169–196
26. Ranieri U, Koza MM, Kuhs WF et al (2017) Fast methane diffusion at the interface of two clathrate structures. Nat Commun 8:1–7
27. Jacobson LC, Hujo W, Molinero V (2010) Amorphous precursors in the nucleation of clathrate hydrates. J Am Chem Soc 132:11806–11811
28. Durham WB, Stern LA, Kirby SH (2003) Ductile flow of methane hydrate. Can J Phys 81:373–380
29. Davidson DW, Handa YP, Ripmeester JA (1986) Xenon-129 NMR and the thermodynamic parameters of xenon hydrate. J Phys Chem 90:6549–6552
30. Waite WF, Gilbert LY, Winters WJ et al (2005) Thermal conductivity of THF hydrate between −25 and +4 °C, and their application to methane hydrate. In: Proceedings of fifth international conference on gas hydrates, pp 1724–1733
31. Christiansen RL, Sloan ED (1994) Mechanisms and kinetics of hydrate formation. Ann N Y Acad Sci 715:283–305
32. Kashchiev D, Firoozabadi A (2002) Nucleation of gas hydrates. J Cryst Growth 243:476–489
33. Li XS, Liu YJ, Zeng ZY et al (2011) Equilibrium hydrate formation conditions for the mixtures of methane + ionic liquids + water. J Chem Eng Data 56:119–123
34. Boyun G, Shanhong S, Ghalambor A (2014) Offshore pipelines design, installation, and maintenance, 2nd edn. Elsevier, p 383
35. Xiao C, Adidharma H (2009) Dual function inhibitors for methane hydrate. Chem Eng Sci 64:1522–1527
36. Sabil KM, Nashed O, Lal B et al (2015) Experimental investigation on the dissociation conditions of methane hydrate in the presence of imidazolium-based ionic liquids. Thermodyn J Chem 84:7–13
37. Xiao C, Wibisono N, Adidharma H (2010) Dialkylimidazolium halide ionic liquids as dual function inhibitors for methane hydrate. Chem Eng Sci 65:3080–3087
38. Bavoh CB, Partoon B, Lal B et al (2016) Effect of 1-ethyl-3-methylimidazolium chloride and polyvinylpyrrolidone on kinetics of carbon dioxide hydrates. Int J Appl Chem 12:6–11
39. Nashed O, Sabil KM, Lal B et al (2014) Study of 1-(2-hydroxyethyle) 3-methylimidazolium halide as thermodynamic inhibitors. Appl Mech Mater 625:337–340
40. Nashed O, Dadebayev D, Khan MS et al (2018) Experimental and modelling studies on thermodynamic methane hydrate inhibition in the presence of ionic liquids. J Mol Liq 249:886–891
41. Khan MS, Liew CS, Kurnia KA et al (2016) Application of COSMO-RS in investigating ionic liquid as thermodynamic hydrate inhibitor for methane hydrate. Procedia Eng 148:862–869
42. Bavoh CB, Lal B, Khan MS et al (2018) Combined inhibition effect of 1-ethyl-3-methylimidazolium chloride + glycine on methane hydrate. J Phys: Conf Ser 1123:012060
43. Bavoh CB, Lal B, Keong LK et al (2016) Synergic kinetic inhibition effect of EMIM-CL + PVP on CO$_2$ hydrate formation. Procedia Eng 148:1232–1238
44. Khan MS, Bavoh BC, Lal B et al (2018) Kinetic assessment of tetramethyl ammonium hydroxide (ionic liquid) for carbon dioxide, methane and binary mix gas hydrates. Recent Adv Ion Liq 9:159–179
45. Bavoh CB, Lal B, Nashed O et al (2016) COSMO-RS: an ionic liquid prescreening tool for gas hydrate mitigation. Chin J Chem Eng 11:1619–1624
46. Sa J-H, Kwak G-H, Lee BR et al (2013) Hydrophobic amino acids as a new class of kinetic inhibitors for gas hydrate formation. Sci Rep 3:2428
47. Bavoh CB, Partoon B, Lal B et al (2016) Methane hydrate-liquid-vapour-equilibrium phase condition measurements in the presence of natural amino acids. J Nat Gas Sci Eng 37:425–434
48. Bavoh CB, Lal B, Osei H et al (2019) A review on the role of amino acids in gas hydrate inhibition, CO$_2$ capture and sequestration, and natural gas storage. J Nat Gas Sci Eng 64:52–71
49. Merey Ş (2017) Drilling of gas hydrate reservoirs. J Nat Gas Sci Eng 35:1167–1179

50. Sami NA, Sangwai J, Subramanian B (2013) Gas hydrate applications and problems in oil and gas industry. Int J Sci Eng Res 4:1–5
51. Fan S, Li S, Wang J et al (2009) Efficient capture of $CO_2$ from simulated flue gas by formation of TBAB or TBAF semiclathrate hydrates. Energy Fuels 23:4202–4208
52. Partoon B, Sabil KM, Roslan H et al (2016) Impact of acetone on phase boundary of methane and carbon dioxide mixed hydrates. Fluid Phase Equilib 412:51–56
53. Partoon B, Malik SNA, Azemi MH et al (2013) Experimental investigations on the potential of SDS as low-dosage promoter for carbon dioxide hydrate formation. Asia-Pac J Chem Eng 8:258–261
54. Deschamps J, Dalmazzone D (2009) Dissociation enthalpies and phase equilibrium for TBAB semi-clathrate hydrates of $N_2$, $CO_2$, $N_2 + CO_2$ and $CH_4 + CO_2$. J Therm Anal Calorim 98:113–118
55. Nashed O, Partoon B, Lal B et al (2018) Review the impact of nanoparticles on the thermodynamics and kinetics of gas hydrate formation. J Nat Gas Sci Eng 55:452–465
56. Veluswamy HP, Kumar A, Seo Y et al (2018) A review of solidified natural gas (SNG) technology for gas storage via clathrate hydrates. Appl Energy 216:262–285
57. Ganji H, Manteghian M, Rahimi Mofrad H (2007) Effect of mixed compounds on methane hydrate formation and dissociation rates and storage capacity. Fuel Process Technol 88:891–895
58. Darbouret M, Cournil M, Herri J-M (2005) Rheological study of TBAB hydrate slurries as secondary two-phase refrigerants. Int J Refrig 28:663–671
59. Sabil KM, Witkamp G-J, Peters CJ (2010) Estimations of enthalpies of dissociation of simple and mixed carbon dioxide hydrates from phase equilibrium data. Fluid Phase Equilib 290:109–114
60. Linga P, Babu P, Nambiar AP (2018) A clathrate hydrate desalination method. WO/2018/156083
61. Nambiar A, Babu P, Linga P (2019) Improved kinetics and water recovery with propane as co-guest gas on the hydrate-based desalination (hydesal) process. Chem Eng 3:31
62. Mannar N, Bavoh CB, Baharudin AH et al (2017) Thermophysical properties of aqueous lysine and its inhibition influence on methane and carbon dioxide hydrate phase boundary condition. Fluid Phase Equilib 454:57–63
63. Bavoh CB, Partoon B, Lal B et al (2017) Inhibition effect of amino acids on carbon dioxide hydrate. Chem Eng Sci 171:331–339
64. Khan MSMS, Bavoh CB, Partoon B et al (2017) Thermodynamic effect of ammonium based ionic liquids on $CO_2$ hydrates phase boundary. J Mol Liq 238:533–539
65. Trueba AT, Radović IR, Zevenbergen JF et al (2012) Kinetics measurements and in situ Raman spectroscopy of formation of hydrogen-tetrabutylammonium bromide semi-hydrates. Int J Hydrogen Energy 37:5790–5797
66. Khan MSMS, Partoon B, Bavoh CB et al (2017) Influence of tetramethylammonium hydroxide on methane and carbon dioxide gas hydrate phase equilibrium conditions. Fluid Phase Equilib 440:1–8
67. Mohammadi AH, Richon D (2010) Gas hydrate phase equilibrium in the presence of ethylene glycol or methanol aqueous solution. Ind Eng Chem Res 49:8865–8869
68. Odutola TO, Ajienka JA, Onyekonwu MO et al (2016) Hydrate Inhibition in laboratory flow loop using polyvinylpyrrolidone, N-Vinylcaprolactam and 2-(Dimethylamino)ethylmethacrylate. J Nat Gas Sci Eng 36:54–61
69. Talaghat MR (2014) Experimental investigation of induction time for double gas hydrate formation in the simultaneous presence of the PVP and l-Tyrosine as kinetic inhibitors in a mini flow loop apparatus. J Nat Gas Sci Eng 19:215–220
70. Sowa B, Zhang XH, Hartley PG et al (2014) Formation of Ice, tetrahydrofuran hydrate, and methane/propane mixed gas hydrates in strong monovalent salt solutions. Energy Fuels 11:6877–6888
71. Tohidi B, Burgass RW, Danesh A et al (2000) Improving the accuracy of gas hydrate dissociation point measurements. Gas Hydrates Chall Futur 912:924–931